SIMULTANEOUS CO-DELIVERY OF NEUROPROTECTIVE DRUGS FROM MULTI-LOADED PLGA MICROSPHERES FOR THE TREATMENT OF GLAUCOMA

Arranz-Romera A[a,c] , Davis BM[b,d], Bravo-Osuna I[a,c], Esteban-Pérez S[a,c], Molina-Martínez

I.T[a,c], Shamsher E[b], Ravindran N[b], Guo, L[b], Cordeiro MF[b,d*], Herrero-Vanrell R[a,c*]

[a]Pharmaceutical Innovation in Ophthalmology (InnOftal). Research Group (UCM 920415), Pharmaceutics and Food Technology, Faculty of Pharmacy, Complutense University, Madrid, Spain.

[b]Glaucoma and Retinal Neurodegeneration Research, UCL Institute of Ophthalmology, London EC1V 9EL, United Kingdom

[c]Red Temática de Investigación Cooperativa Sanitaria en Enfermedades Oculares (Oftared) e Instituto de Investigación Sanitaria del Hospital Clínico San Carlos (IdISSC).

[d] Imperial College Ophthalmology Research Group (ICORG), Western Eye Hospital, Imperial College London, United Kingdom.

*Corresponding authors:

Rocío Herrero-Vanrell, Department of Pharmaceutics and Food Technology, Faculty of Pharmacy, Pza. Ramón y Cajal s/n, 28040 Madrid, Spain. E-mail address: rociohv@farm.ucm.es.

M. Francesca Cordeiro, Department of Visual Neuroscience, UCL Institute of Ophthalmology, London EC1V 9EL, United Kingdom. E-mail address: m.cordeiro@ucl.ac.uk

Graphical abstract:
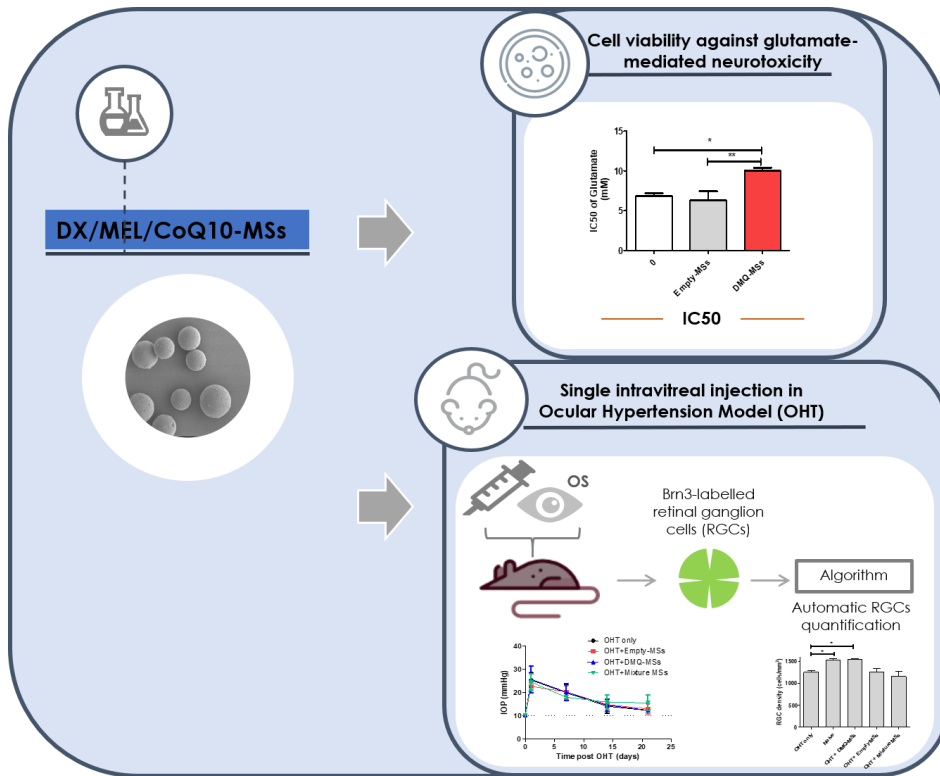
Abstract

Glaucoma is a multifactorial neurodegenerative disorder and one of the leading causes of irreversible blindness globally and for which intraocular pressure is the only modifiable risk factor. Although neuroprotective therapies have been suggested to have therapeutic potential, drug delivery for the treatment of ocular disorders such as glaucoma remains an unmet clinical need, further complicated by poor patient compliance with topically applied treatments. In the present study we describe the development of multi-loaded PLGA-microspheres (MSs) incorporating three recognised neuroprotective agents (dexamethasone (DX), melatonin (MEL) and coenzyme Q10 (CoQ10)) in a single formulation (DMQ-MSs) to create a novel sustained-release intraocular drug delivery system (IODDS) for the treatment of glaucoma. MSs were spherical, with a mean particle size of 29.04 ± 1.89 µm rendering them suitable for intravitreal injection using conventional 25G-32G needles. Greater than 62% incorporation efficiency was achieved for the three drug cargo and MSs were able to co-deliver the encapsulated active compounds in a sustained manner over 30-days with low burst release. *In vitro* studies showed DMQ-MSs to be neuroprotective in a glutamate-induced cytotoxicity model (IC$_{50}$ 10.00±0.94 mM *versus* 6.89±0.82 mM in absence of DMQ-MSs) in R28 cell line. *In vivo* efficacy studies were performed using a well-established rodent model of chronic ocular hypertension (OHT), comparing single intravitreal injections of microspheres of DMQ-MSs to their equivalent individual single-drug loaded MSs mixture (MSsmix), empty MSs, no-treatment OHT only and naïve groups. Twenty one days after OHT induction, DMQ-MSs showed a significantly neuroprotective effect on RGCs compared to OHT only controls. No such protective effect was observed in empty MSs and single-drug MSs treated groups. This work suggests that multi-loaded PLGA MSs present a novel therapeutic approach in the management of retinal neurodegeneration conditions such as glaucoma.

Keywords: Intraocular Drug Delivery, Poly lactic-co-glycolic acid (PLGA), Neuroprotection, *In vivo* efficacy, Glaucoma, Co-delivery, Combination therapy

1. Introduction

Glaucoma is a multifactorial neurodegenerative disorder and one of the leading causes of irreversible blindness worldwide [1]. While this condition is primarily characterised by the loss of retinal ganglion cells (RGCs) and the gradual degeneration of RGC axons in the optic nerve [2], recent morphological and functional studies have suggested the involvement of other retinal cell types, including atrophic changes in the photoreceptor layer and microglia activation [3-5]. At present, intraocular pressure (IOP) is the major clinically modifiable risk factor for glaucoma progression (vision loss) and current therapies seek to modulate IOP via reducing aqueous production or increasing outflow [6]. With the recognition that glaucoma patients can continue to progress despite well controlled IOP, new therapeutic paradigms for the treatment of this condition are being sought [7, 8]. One such approach is neuroprotection which is defined as a "therapeutic approach" aiming to directly prevent, hinder and, in some cases, reverse neuronal cell damage.[9] In glaucoma, this translates to non-IOP-dependent treatments that reduce the rate of RGCs loss and therefore preserve vision [10, 11]. To date, multiple neurodegenerative processes have been implicated in glaucomatous RGC loss, including: glutamate excitotoxicity, inflammation, mitochondrial dysfunction, oxidative stress, aggregation of misfolded proteins, neurotrophic deprivation, ischemia and axonal transport dysregulation [12-14]. Moreover, it is becoming clear that these events can interact and compound, suggesting that effective treatment of glaucoma may require a multi-modal approach [15, 16].

At present, the majority of glaucoma therapies are administered topically as eye drops; however, poor ocular penetration of topically applied drugs to the posterior ocular segment combined with variable patient compliance limit the utility of this approach[17]. Intraocular injection overcomes both these aspects, but this method of administration is

invasive, expensive, burdensome to deliver and associated with small though significant risks of complications[18]. Moreover, the short half-life values of the active substances in the vitreous makes necessary the use of repeated intravitreal injections[19]. Depending on the size, intraocular drug delivery system (IODDS) are classified as nanocarriers (1–1000 nm), microcarriers (1–1000 µm), and implants (>1 mm). The choice of the most convenient IODDS depends on the target site, the ophthalmic disease and the duration of the treatment. While implants and microcarriers have received a lot of interest because they can provide long-term delivery of the active substance, nanocarriers have the advantage to be internalised by cells being highly useful for gene therapy [20]. IODDS based on biodegradable particulate carrier systems have been extensively investigated for the sustained release of therapies to address these problems. Poly(lactide-co-glycolide) acid (PLGA) is approved by the FDA and European Medical Agency for use in intraocular devices [17, 21]. Among the different IODDS, microspheres (MSs) have recently gained considerable attention for ocular applications [22]. These controlled-release drug microsystems can be administered as suspensions using conventional 25G-32G needles. Moreover, repeated administration is reduced as IODSS can sustain therapeutic drug concentrations in target tissues for extended periods [20]. IODDS can additionally be used to personalize therapy by titrating the amount of administered MSs with individual need. The authors postulate that the employment of physical mixtures of different drug loaded-MSs would enable the treatment of more than one therapeutic target simultaneously. A recent published study from our group, however, reported that there is an upper limit to the amount of MSs that can be injected intravitreally; 0.5 mg of PLGA-MSs was found to induce retinal stress and photoreceptor dysfunction in rodents, a phenomenon not observed on administration of 0.1 mg of MSs [23]. To reduce the amount of carrier administered, we have since developed MSs co-delivery systems able to incorporate and control the release of multiple active substances from a single carrier[24].

The present study describes a MSs formulation incorporating three established therapies with anti-inflammatory and neuroprotective activity; dexamethasone, melatonin and coenzyme Q10. The corticosteroid dexamethasone (DX) is commonly used in the treatment of ocular inflammation in conditions such as diabetic macular edema, central retinal vein occlusion, and uveitis [25-27]. Melatonin (MEL) is an antioxidant with free radical scavenging and neuroprotective activity mediated via multiple mechanisms including the inhibition of the mitochondrial transition pore, reducing NO-induced apoptosis or reducing excitotoxicity Ca^{2+} overload [28-31]. Coenzyme Q10 (ubiquinone, CoQ10), an essential cofactor of the electron transport chain, is known for its key role in mitochondrial bioenergetics by maintaining the membrane potential, supporting ATP synthesis and inhibiting reactive oxygen species generation [32-36].

In the present work, we sought to evaluate the effect of a MSs drug co-delivery system (DX, MEL and CoQ10) *vs* an equivalent physical mixture of single drug loaded MSs on RGC survival using the well-established Morrison's rodent model of ocular hypertension. *In vivo* study sought to produce, characterise and evaluate the ability of novel combinations of established neuroprotective therapies to preserve RGC populations. Endpoints in this study included in vitro cell viability and whole-retinal histological assessments of RGC population. The *in vitro* neuroprotective activity of DMQ-MSs formulations were assessed using an *in vitro* glutamate-mediated neurotoxicity model in an immortalised and rat derived neuronal cell line (R28)[37].

While induction of the Morrison's rodent model requires advanced microsurgical skills, it yields the following advantages compared to episcleral vein ligation models, including: (i) the establishment of anterior chamber deepening consistent with aqueous humor outflow obstruction, something not observed in episcleral vein ligation models.[38], (ii) reduced rate of IOP elevation [39], and (iii) reduced risk of ischemic injury[38].

To the authors knowledge, this is the first co-delivery study of three neuroprotective active substances in an IODDS administered to the posterior ocular segment.

2. Materials and methods

Dexamethasone, melatonin and coenzyme Q10 were supplied by Sigma-Aldrich (St. Louis Mo., USA) at the highest available purity. Poly(D,L-lactide-co-glycolide) (PLGA) 50:50 (Mwt 35,000 g/mol) was purchased from Evonik España (Granollers, Spain). Polyvinyl alcohol 67,000 g/mol (PVA) was supplied by Merck KGaA (Darmstadt, Germany). Isopropyl alcohol, methanol and acetonitrile, HPLC grade (PanReac AppliChem, Barcelona, Spain) were used to prepare the mobile phases in HPLC determinations. All other chemicals were reagent grade and used as received.

2.1 Manufacture of PLGA Microspheres

PLGA microspheres (MSs) containing three neuroprotective agents (dexamethasone (DX), melatonin (MEL) and coenzyme Q10(CoQ10), 2/1/0.5:10) (DMQ-MSs) were prepared by the Oil/Water emulsion solvent extraction-evaporation technique (Fig.1). Briefly, CoQ10 (20 mg) and PLGA (400mg) were first dissolved in 0.7 mL of methylene chloride. 80 mg DX and 40 mg MEL were then ground in a pestle and mortar before dispersing in the organic PLGA solution by ultrasonication in an ice-water bath (Ultrasons; J.P. Selecta, Barcelona, Spain) for 5 minutes, followed by sonication (Sonicator XL; Heat Systems, Inc., Farmingdale, NY, USA) for 1 minute at 4 °C. Finally, the resulting organic phase was emulsified with 5 mL of polyvinyl alcohol (PVA) MiliQ water solution (1% w/v) in a homogenizer (Polytron®RECO, Kinematica, GmbHT PT3000, Lucerna, Swithzerland, 8,500rpm for 2 min). The first emulsion was then combined with 100 mL of an aqueous PVA solution (0.1%w/v) with magnetic stirred for 3 hours at room temperature to facilitate organic solvent evaporation. After maturation, the formed MSs were washed in distilled water to remove PVA and separated according to their particle size (38-20 μm) by filtration using two sieves (mesh size: 38 and 20 μm). Finally, MSs were lyophilised (Freezing: -60ºC /15 min, Primary drying: -40 ºC/12h/0.1

mBar, Secondary drying: 20 ºC/2h/0.1 mBar) and resulting cakes stored at -20 ºC under dry conditions until required. In addition, MSs loaded with each single drug DX: PLGA (2:10), MEL:PLGA (1:10) and CoQ10:PLGA (0.5:10) and empty MSs in the absence of drug cargo were prepared using the same protocol.
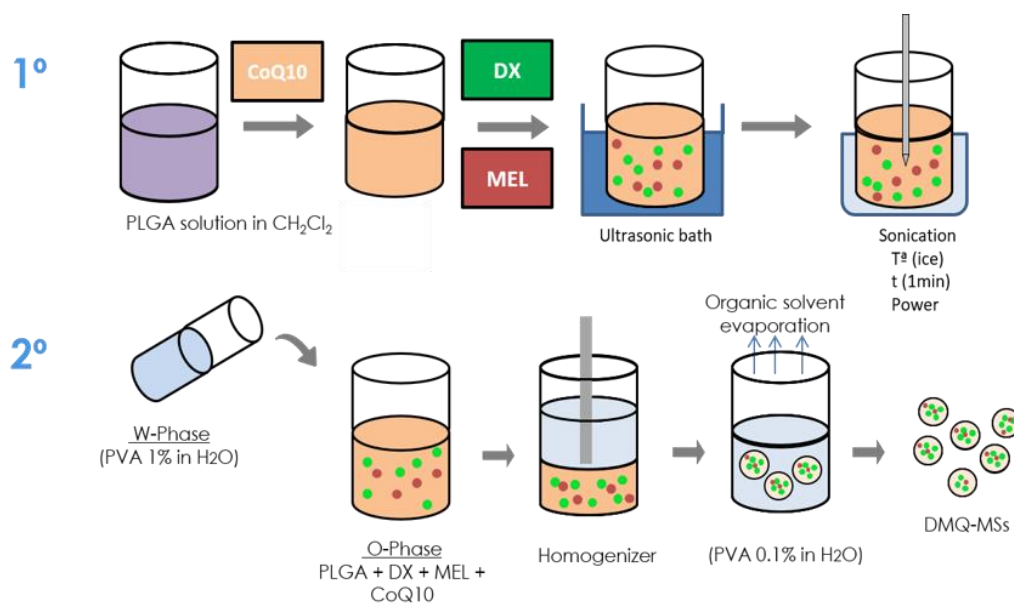

Figure 1. Elaboration process of the mullti-loaded MSs.

2.2. Dexamethasone/melatonin/coenzyme Q10 quantification by LC/MS

The LC/MS system comprised a Waters LC instrument (Waters 2707 autosampler and Waters 1525 binary HPLC pump) with a Nova-Pak C18 column (4µm, ID 2.1 mm×150 mm) with a C18 guard column (3.9 mm ×20 mm), connected to a Waters 3100 single quadrupole mass spectrometer via Empower 2 (Waters, Milford, USA). The analytical column temperature was maintained at 45 ˚C. For MSs detection, the ESI source was operated in the positive ion mode (ESI(+)). Selected ion recordings (SIR) CoQ10 mass (m/z) 197, MEL mass (m/z) 174.2 and DX masses (m/z) 393.40 and 147.10 were obtained with the following mass spectrometer source conditions of 3.5 kV electrospray voltage and 130 °C heated capillary temperature. Nitrogen gas (>99.999%) was used for

nebulization (100 L/h flow rate, 130 °C source temperature, 5 V extractor voltage) and desolvation (400 L/h flow rate, 300 °C desolvation temperature).

Two different isocratic HPLC methods were developed to quantify drug entrapment efficiencies (method A) and drug release from MSs (method B). Method A was composed of 50% of 10 mM ammonium acetate/1mL formic acid in methanol and 50% of 10 mM ammonium acetate/1mL formic acid in isopropyl alcohol (flow rate, 0.3 mL/min) and method B 60% of 10 mM ammonium acetate/1mL formic acid in water and 40% of acetonitrile (flow rate, 0.3 mL/min).

2.3. Microspheres characterization

MSs were characterised in terms of production yield (%), mean particle size and size distribution, morphological evaluation, encapsulation efficiency, *in vitro* release studies and DSC Analysis.

2.3.1. Production yield percentage

The yield percentage (PY%) of each batch was calculated according to the following equation (1):

$$PY\% = \frac{\text{Weight of MSs (W}_1)}{\text{Total weight of active substances and polymer (W}_2)} \times 100$$

[Eq.1]

2.3.2. Mean particle size and particle size distribution

Particle size and the particle size distribution was measured by light scattering Microtrac® S3500 Series Particle Size Analyzer, Montgomeryville, PA, USA). The mean particle sizes, expressed as volume mean diameters, and standard deviation were determined. Each sample was run in triplicate.

2.3.3. Morphological evaluation

The external morphology of the freeze-dried microspheres was observed by scanning electron microscopy (SEM, Jeol, JSM-6335F, Tokyo, Japan). Samples were gold sputter-coated prior to observation. The internal morphology of MSs was examined using thickness slides (70 nm) of cross-section by transmission electron microscopy (TEM, Jeol, JEM-1010, MA, USA). A Leica Cryostat CM 1900 was employed to create the cross-sections of microspheres at -20 ^{0}C placed into a synthetic resin medium (Spurr Low Viscosity Embedding Kit).

2.3.4. Encapsulation efficiency

The determination of the drug entrapment efficiencies was quantified as follows: 1 mg of MSs was dissolved in 2.5 mL of methylene chloride, following which drugs were extracted with methanol (6 mL), which also promoted polymer precipitation. After vortex mixing, the samples were centrifuged (5,000rpm for 5 minutes at 20ºC) and the methanolic supernatant was recuperated and filtered (0.22μm). High-Performance Liquid Chromatography-mass spectrometry (HPLC-MS) was employed for active substance quantifications according to the method described previously (Method A).

2.3.5. In vitro release studies

5 mg of MSs (DX-loaded MSs, MEL-loaded MSs and DMQ (Dexamethasone/Melatonin/Coenzyme Q10)-loaded MSs) were suspended in 2 mL of release medium (phosphate buffer saline (PBS, pH 7.4) with sodium azide (0.02%)) in duplicate and placed in a water shaker bath under constant agitation (100 rpm) at 37ºC (Memmert Shaking Bath, Memmert, Schwabach, Germany). At specified timepoints (1, 2, 4, 7, 10, 14, 17, 21, 24, 28 and 30 days) samples were centrifuged (5,000 rpm for 5 min, 20ºC) and the supernatants removed and replaced by the same volume of fresh

media. After filtration (0.22μm), drug concentrations in the release media were measured by LC/MS, according to the aforementioned method.

Due to the poor aqueous solubility of CoQ10, the release profile of this drug was determined as the difference between initial encapsulation efficiency and the concentration remaining incorporated within the MSs at each sampling time. Here, 22 samples of CoQ10-loaded MSs and DMQ-loaded MSs (4mg) were suspended in 2 mL of release medium and kept under a constant agitation at 37ºC. At the specified time points MSs suspensions were centrifuged (8,500 rpm; 3 min; 20 ºC) and the supernatants removed, and particles freeze-dried. Subsequently, the amount of CoQ10 was quantified according to the aforementioned encapsulation efficiency method.

2.3.6. DSC Analysis

Thermal analysis of starting materials, empty and drug loaded MSs were carried out by means of a Mettler differential scanning calorimeter (DSC820, Toledo Mettler Laboratory & Weighing Tech., Greifensee, Suiza) equipped with a TAC 7/DX instrument controller. A STAR^e SW9.10 system software was used for the data acquisition. A heating rate of 10 ºC/min in heating-cooling-heating cycle (25-100ºC/100-25ºC/25-280ºC temperature ranges) was employed and an empty aluminium pan (Mettler) was used as a reference standard. Analysis were performed on 5 mg samples under nitrogen purge.

2.4. Cell culture

R28 cell line (Kerafast, Boston, MA) was cultured in Dulbecco's modified Eagle's medium (DMEM; Invitrogen, Paisley, UK) supplemented with 5% heat-inactivated foetal bovine serum (Invitrogen, UK), 100 U/ml penicillin, 100μg/ml of streptomycin and 0.292 mg/mL glutamine (Gibco, UK), 7.5% sterile dH20 and 1.5 mM KCl (Sigma-Aldrich, UK). Cells

were maintained under standard conditions: $37^{\circ}C$, 5% CO_2, 100% humidity, medium was changed completely every other day and cultures were passaged at 90% confluence.

2.4.1. Cell viability assessment

R28 cells were seeded at 4,000 cells/well in 96-well plates for 24 h before treatment with varying concentrations of the three active substances (DX, MEL, CoQ10), individually or in the form of a multiloaded MSs formulation and appropriate vehicle controls for a second 24h period. During this second 24h period, cells were additionally exposed to varying concentrations of the cytotoxic insult Glutamate (Sigma-Aldrich, UK). After this time, cell viability in the presence/absence of each therapy and insult was assessed by Alamarblue (Invitrogen, UK) assay according to manufacturer's instructions. Briefly, the Alamarblue solution (10% v/v) was added to each well and incubated for 4 h at 37 °C. A Safire plate reader (excitation of 530 nm and emission of 590 nm) was used for the fluorescence measurement and determination of percentage cell viability as previously described [36]. All experiments were completed in triplicate.

2.5. Animals

Adult male Dark Agouti (150-200g, Harlan Laboratories, UK) rats were housed in a temperature (21ºC) and humidity-controlled environment with a 12 h light-dark cycle (140–260 lux). Water and food were available *ad libitum*. All procedures described were performed in agreement with the ARVO Statement for the Use of Animals in Ophthalmic and Vision Research and under protocols approved by the U.K. Home Office.

2.5.1. Ocular hypertension model

IOP elevation was performed in the left eyes of twenty-five Dark Agouti rats by episcleral injection of hypersaline solution as previously described (Morrison's ocular hypertension

model)[40]. On the day of glaucoma induction, IOP measurements were performed in both eyes with a TonoLab tonometer (Tiolat Oy, Helsinki, Finland). Subsequently, the animals received general anesthesia using a mixture of 37.5% Ketamine (Pfizer Animal Heath, Exton, PA), 25% Dormitol (Pfizer Animal Heath, Exton, PA) and 37.5% sterile water, at 2 mL/kg administered intraperitoneally. To elevate the IOP, a syringe pump (50µL/min; UMP2; World Precision Instruments, Sarasota, FL, USA) was used to inject 50 µL of hypertonic saline solution (1.85 M) into the two episcleral veins. A propylene ring with a 1 mm gap cut from the circumference was placed around the equator to prevent injected saline outflow from other aqueous veins. Once a week, the IOP from both eyes of each rat was measured at regular intervals using a TonoLab tonometer (Tiolat Oy, Helsinki, Finland) under inhalational anaesthesia (0.4% isoflurane inoxygen) until 21 days post unilateral IOP elevation. For each animal, cumulative IOP exposure, defined as the integral of IOP elevation over time (mm Hg/day), was calculated from the area under the curve, as previously described[41].

2.5.2. Microspheres administration

Animals were randomized into 5 treatment groups (n = 5 each): non-loaded PLGA MSs (Empty-MSs, 5.825% w/v), multiloaded MSs (DMQ-loaded MSs, 2.5% w/v), the physical mixture of each single drug loaded MSs (DX-loaded MSs, MEL-loaded MSs and CoQ10-loaded MSs, MSsmix, 5.825% w/v), OHT-untreated and naïve controls (Table 1).

Table 1
Suspensions of administered MSs

	DMQ-loaded MSs	Physical Mixture of MSs			Empty-MSs
		DX-MSs	MEL-MSs	CoQ10-MSs	
AMOUNT OF MSs (mg)	0.1	0.071	0.082	0.08	0.233
			0.233		
DOSES (µg drug)	DX / MEL /CoQ10 11.5 / 4.6 / 3.6	DX 11.5	MEL 4.6	CoQ10 3.6	-
VOL. INYECTED (µL)	4		4		4
MSs suspension (w/v) %	2.5		5.825		5.825

The amount of MSs loaded with each single drug injected in the physical mixture was calculated in order to administer the same dose of the active substances (DX, MEL and CoQ10) included in the multiloaded formulation. Similarly, the amount of MSs in the Empty-MSs was equivalent to the highest dose of MSs injected.

Homogeneous suspensions of MSs were prepared in PBS and briefly vortexed immediately prior to each injection. Intravitreal injections of microspheres were administered under general anaesthesia and aseptic conditions before IOP elevation surgery in left eyes of 15 rats, with no treatment given to 5 OHT-only and 5 bilaterally naïve animals.

A 30-gauge hypodermic needle was used to perforate the sclera 1.5 mm behind the limbus. Four microliters of sample were then injected into the vitreous using a 5 µL Hamilton Syringe (Hamilton Co, Reno, NV). To prevent backflow of MSs, the needle was left in place for a short while and withdrawn slowly. Animals were euthanized 23 days post-surgery.

2.5.3 Brn3a immunohistochemistry and confocal microscopy

After animals were sacrificed, enucleated eyes were fixed in 4% paraformaldehyde at 4ºC overnight before dissecting retinal whole mounts. Brn3a+ RGCs were labelled as previously described [41]. Briefly, RGCs were labelled using an anti-mouse mAb (1:750; Merk Milipore, Darmstadt, Germany) and as secondary detection donkey anti-mouse IgG(HbL)-Alexa 647 (1:200; Merk Milipore, Darmstadt, Germany). Subsequently, retinas were examined under confocal microscopy (LSM 710; Carl Zeiss MicroImaging GmbH, Jena, Germany). Whole-mounts were imaged as a tiled z-stack at ×10 magnification, which was used to generate a single plane maximum projection of the RGC layer in each retina for subsequent analysis. Each whole-mount image was manually orientated so

that the superior retina was towards the top of the image using *in vivo* cSLO imaging of retinal vasculature as a reference. Retina image acquisition settings were kept constant for all retinas imaged, allowing comparison of Brn3a expression in each experimental group as previously described [42]. Automated quantification of Brn3a labelled RGCs in retinal whole mounts was completed as described previously [41].

2.6. Statistical analysis

All data were represented as mean ± standard deviation (SD) or mean ± standard error (SE). Linear regression analysis was completed using R version 3.3.1. $P < 0.05$ was considered statistically significant.

3. Results

3.1. Microspheres characterization

SEM investigation confirmed the presence of spherical particles with comparable and regular size distributions. Surface morphological differences was observed between formulations. Non-loaded MSs, MEL-loaded MSs and DX-loaded MSs had a smooth appearance with only small imperfections visible in the case of loaded MSs. In contrast, CoQ10-loaded MSs exhibited a number of small pores with a rough surface. The microspheres formulation prepared with the three active compounds (DMQ-loaded MSs) showed similar porous and rough surfaces (Fig.2).

TEM images of the fractured microspheres revealed a non-interconnected pore architecture inside the internal polymeric matrix. Compared to non-loaded MSs, the formulations loaded with actives substances presented big hollows in the inner structure. Thus, DX-loaded MSs inner structure showed solid particles consistent with dexamethasone crystals. MEL-loaded MSs presented a homogeneous porous composition whereas CoQ10-loaded MSs showed irregularly distributed large pores. The internal appearance of DMQ-loaded MSs revealed a combination of all three aspects (Fig.2).
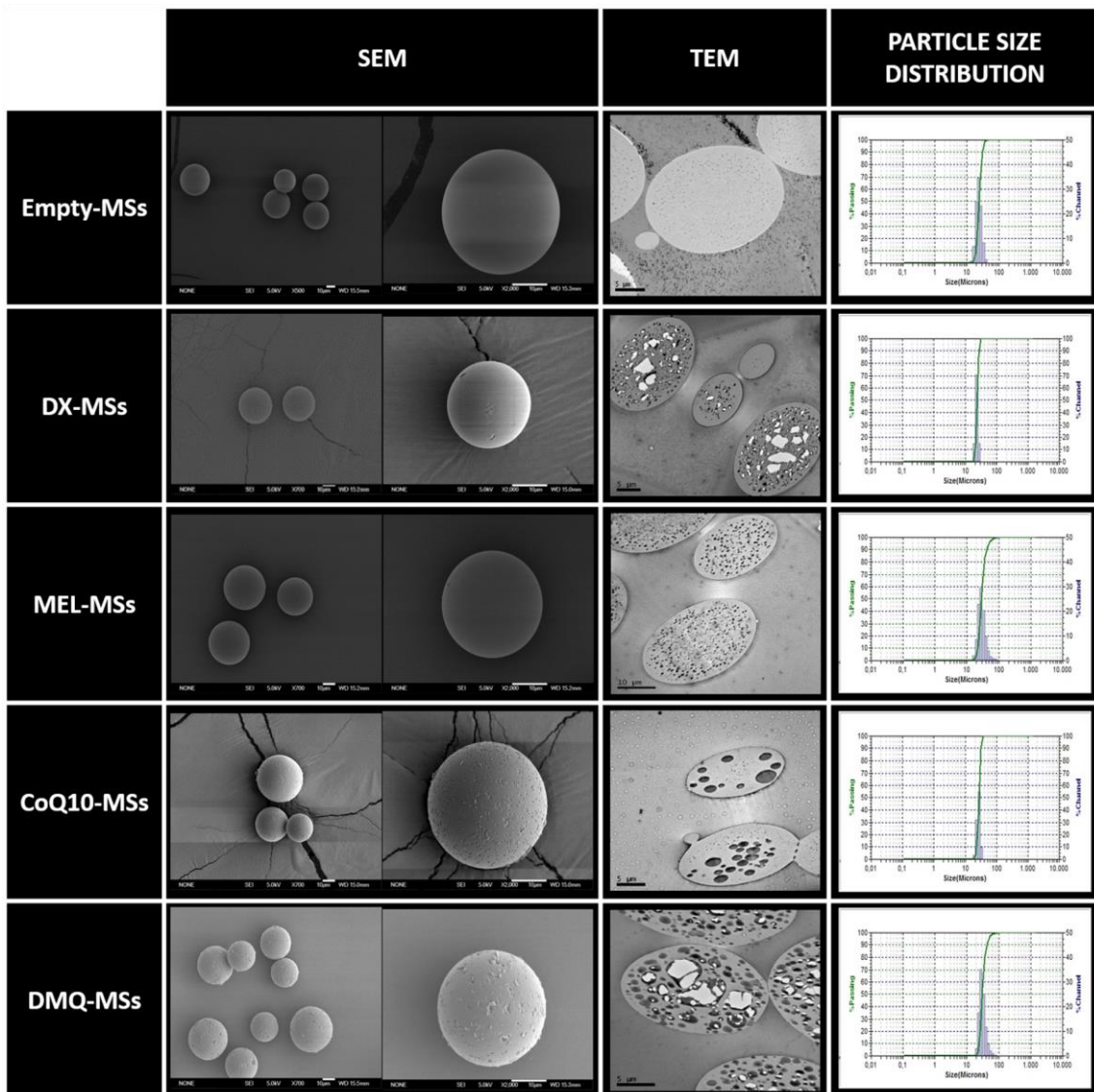
Figure 2. Morphological evaluation (Scanning electron microscopy and Transmission electron microscopy) and particle size distribution.

The MSs microencapsulation technique led to a high production yield (> 72% in all cases) with mean particle for the multiloaded and single loading formulations ranging from 24 to 29 μm as outlined in Table 2.

3.1.1 Encapsulation efficiency

Table 2 summarizes the encapsulation efficiency data for each formulation. DX encapsulation efficiency in the multiloaded MSs (78.20 ± 0.42 %) was reduced compared to the single one drug formulation (97.49 ± 1.53 %) suggesting some competition for

drug loading sites. In contrast, MEL and CoQ10 encapsulation efficiencies remained the same values in both formulations (~62% and ~96% respectively).

Table 2
Production yield, mean particle size and encapsulation efficiency data for each formulation. Data are shown as mean ± SD.

FORMULATION	PRODUCTION YIELD (%)	MEAN SIZE (µm)	ENCAPSULATION EFFICIENCY					
			µg DX/mg MSs	µg MEL/mg MSs	µg Q10/mg MSs	EE DX (%)	EE MEL (%)	EE CoQ10 (%)
Empty-MSs	85.97±3.46	24.72±0.79	-	-	-	-	-	-
DX-MSs	86.62±3.85	24.50±1.76	162.49±2.55	-	-	97.49±1.53	-	-
MEL-MSs	86.41±1.55	27.46±0.66	-	56.52±1.34	-	-	62.17±1.47	-
CoQ10-MSs	75.15±3.23	29.97±1.81	-	-	45.56±1.85	-	-	95.66±3.87
DMQ-MSs	72.99±0.60	29.04±1.89	115.86±0.62	45.80±1.86	35.71±1.53	78.20±0.42	61.83±2.51	96.42±4.12

3.1.2. Release studies

Currently, the drug delivery research is focused on developing systems enable to maintain drug concentrations above the minimum effective level and below the maximum safe concentration for an extended period of time [43, 44]. Thus, the ultimate goal of the development of IODDS for the treatment of retinal diseases and other intraocular pathologies is to obtain long-acting injectable drug formulations with specific control of the release rate and a sustained effect into the target tissue [19, 45]. In the present work, the three active agents were released *in vitro* from the developed formulations in a controlled fashion up to the end of the assay (30 days).

Figure 3 presents the release profile of each single loaded formulation (3A-C) and the release profile of each drug in the DMQ loaded MSs (3D). In the single loaded particles, the amount of dexamethasone *in vitro* released from DX-loaded MSs during the first 24 h (burst) represented 1.83 ± 0.06 % (2.97 ± 0.05 µg DX/mg MSs) of the encapsulated drug. After this low initial delivery, a sustained delivery was observed, with a release rate of 0.26 ± 0.02 µg DX/mg MSs/day from day 1 to day 24, increasing to 1.64 ± 0.30 µg DX/mg MSs/day from day 24 to day the end of the study (day 30) (Fig 3A). The amount of MEL released from MEL-loaded MSs within 24 hours (burst) represented 22.53 ± 0.74

% (12.73 ± 0.12 µg MEL/mg MSs) of the encapsulated drug. After this initial burst, a relatively rapid drug delivery occurred during the first 10 days (4.30 ± 3.96 µg MEL/mg MSs/day). Subsequently, the MEL release rate resulted lower (0.13 ± 0.15 µg MEL/mg MSs/day) from day 10 to day 30 (Fig 3B). Finally, CoQ10-loaded MSs showed a sustained release of the CoQ10 at a rate of 0.35 µg/mg MSs/day during the 30-day study. No burst effect was observed (Fig. 3C).

Release profile of the multiloaded-MSs formulation (DMQ-loaded MSs) exhibited an initial burst of DX of 3.78 ± 0.71% (DX 4.38± 0.80 µg DX/mg MSs), followed by a release rate of 0.60 ± 0.04 µg DX/mg MSs/day until day 24 and 1.20 ± 0.15 µg DX/mg MSs/day from day 24 to day 30. Regarding MEL release, after a burst effect of 28.27± 3.59% (12.91± 1.12 µg MEL/mg MSs), a biphasic release occurred with a rate of 1.66± 0.31 µg MEL/mg MSs/day for the first 14 days and 0.69 ± 0.18 µg MEL/mg MSs/day until day 30. Finally, DMQ-loaded MSs presented a controlled release of the CoQ10 at a rate of 0.63 µg Coenzyme Q10/mg MSs/day during the study (Fig. 3D).
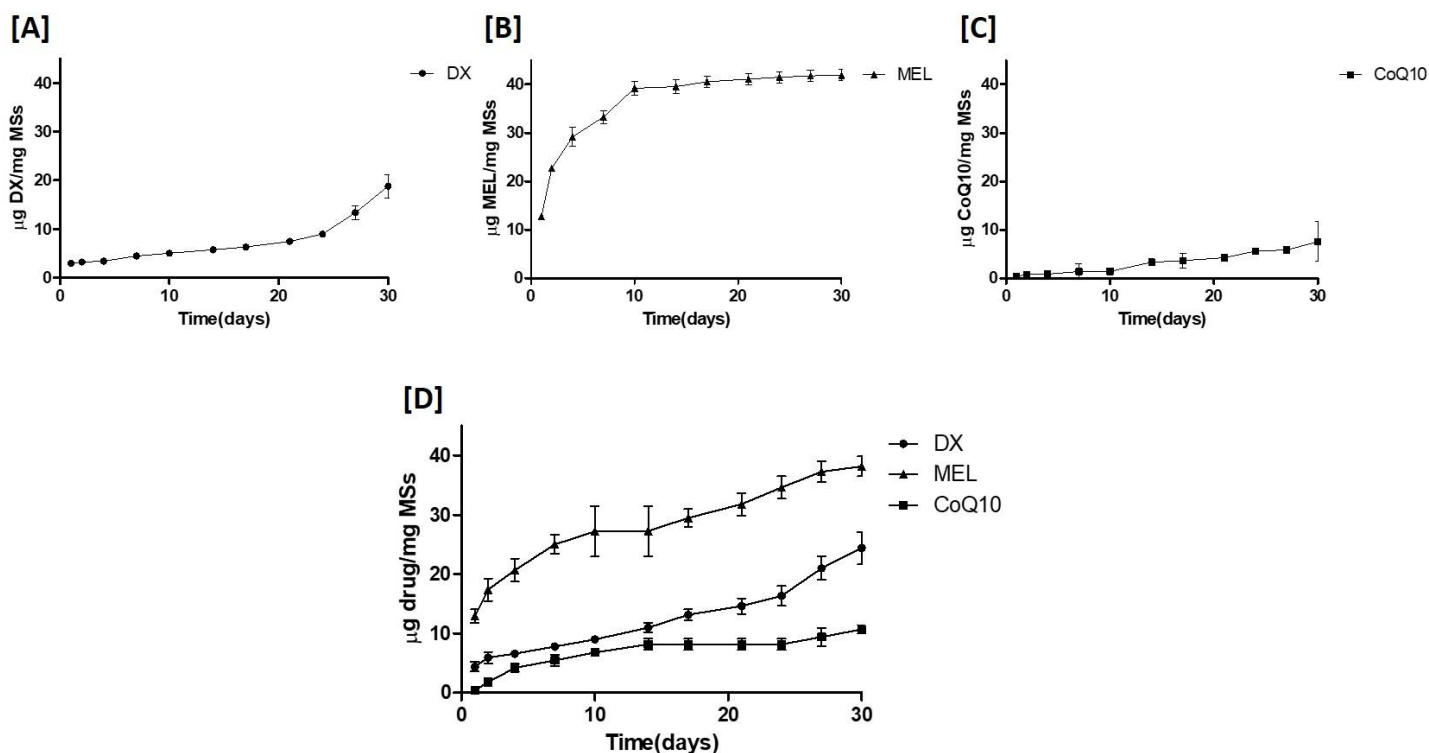

Figure 3. Cumulative *in vitro* release (µg/mgMSs) of DX from DX-loaded MSs [A], MEL from MEL-loaded MSs [B], CoQ10 from CoQ10-loaded MSs [C] and DX, MEL, CoQ10 from DMQ-loaded MSs [D] over one month. Release media: PBS (pH7.4) and 0.02%Na azide.

3.1.3. DSC measurements

DSC scans, which provide qualitative information about the physical status of the drugs in each system, are provided in Figure 4. The thermograms of pure active substances (DX, MEL and CoQ10) displayed sharp endothermic transitions at 244, 118 and 55 ºC respectively, corresponding to their melting points (Fig. 4A). These peaks are also detected in the physical mixture (drugs plus PLGA) (Fig. 4B) whereas they decreased or disappeared in the loaded MSs containing the same fractions of drugs as the physical mixture indicating successful encapsulation (Fig. 4C and 4D).
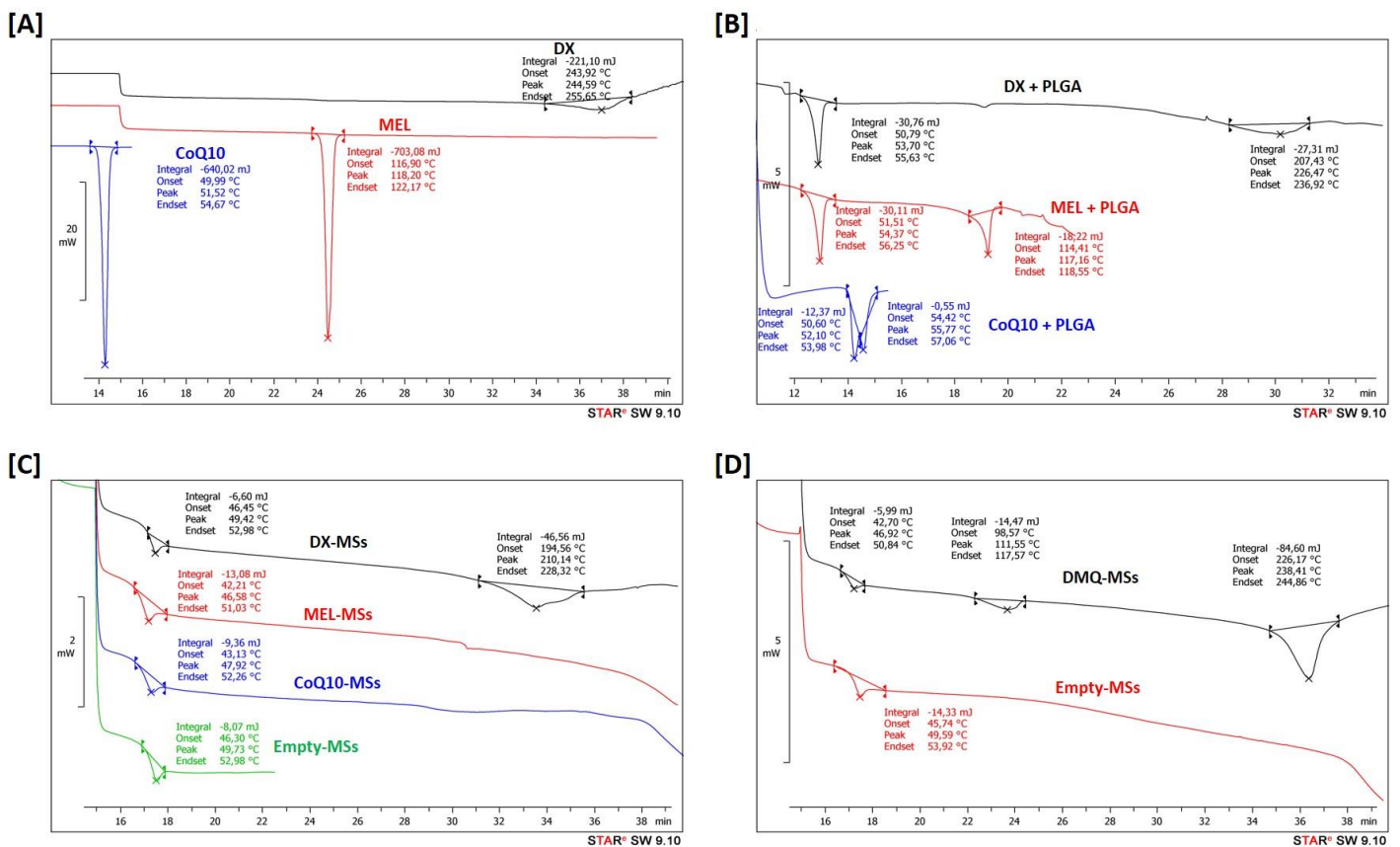

Figure 4. [A] DSC curves of DX, MEL, CoQ10. [B] DSC curves of physical mixture of DX+PLGA, MEL+PLGA, CoQ10+PLGA. [C] DSC curves of DX-MSs, MEL-MSs, CoQ10-MSs and Empty-MSs. [D] DSC curves of DMQ-MSs and Empty-MSs.

3.2. DX/MEL/CoQ10-loaded MSs are neuroprotective in vitro against established model of excitotoxicity-mediated neurotoxicity in R28 retinal cultures.

An *in vitro* model of glutamate-mediated neurotoxicity in R28 cells was used to evaluate the neuroprotective activity of varying concentrations of the three active substances (DX (50 μM, 100 μM,200 μM), MEL (250 μM, 500 μM, 750 μM), CoQ10 (1 μM, 10 μM, 25 μM)) and vehicle controls. Data were fit in dose-response curves to determine the IC_{50} values. Figure 5 illustrates that while the treatment of cells with DX did not elicit a significant neuroprotective effect in this cytotoxic model (Fig. 5A), MEL (500 μM and 750 μM) was neuroprotective compared to control (one-way ANOVA with Tukey posthoc test, p = 0.0012) (Fig. 5B). Also, CoQ10 (10 μM and 25 μM) promoted a significant reduction in cell death induced by glutamate (one-way ANOVA with Tukey posthoc test, p =0.0012) (Fig. 5C).

20 mg/mL of DMQ-loaded MSs (burst initial: 108.5 μM DX, 555.9 μM MEL and 4 μM CoQ10), but not non-loaded MSs, provided protection against the excitotoxic agent insult (glutamate) in R28 cell cultures. Treatment of R28 with the multiloaded MSs significantly reduced the susceptibility of these cells to glutamate-induced cytotoxicity (one-way ANOVA with Tukey posthoc test, *p* = 0.0061) (Fig.5D and 5E).
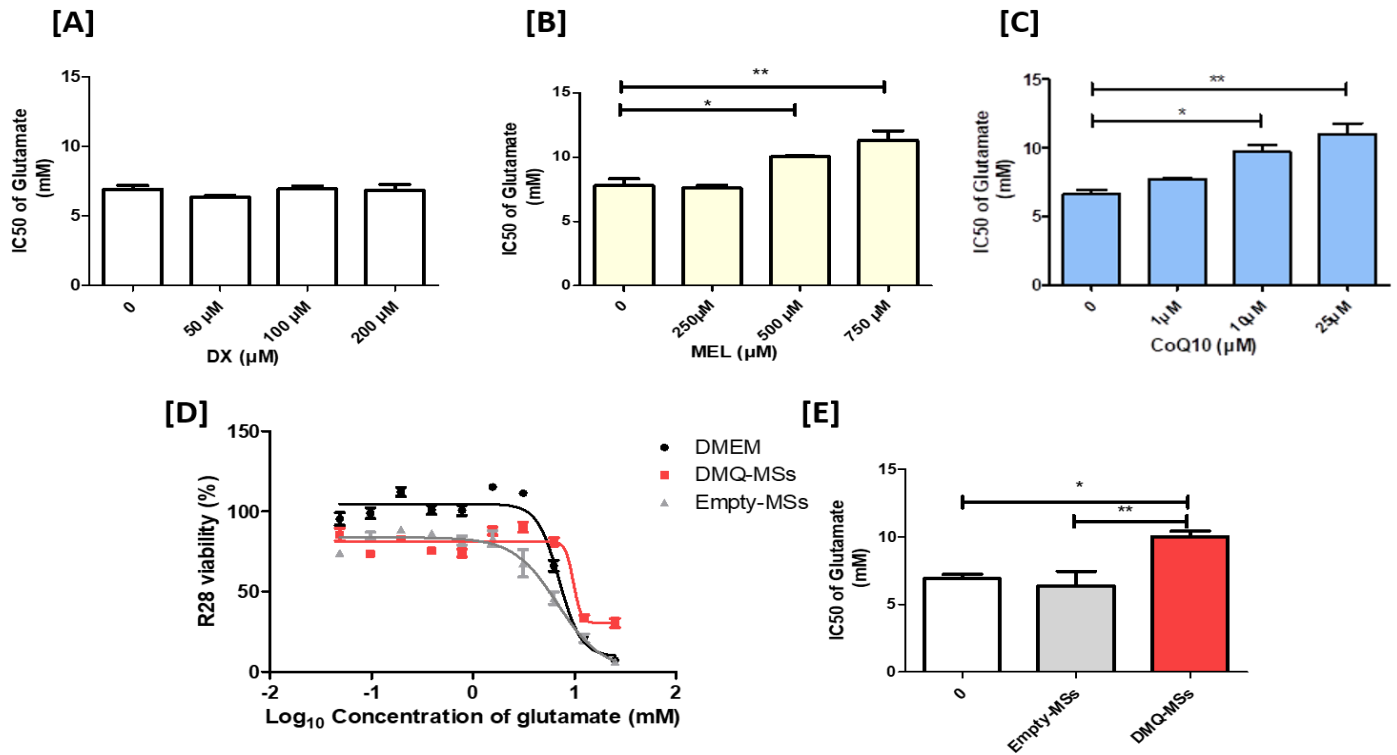
Figure 5. [A-C] MEL (500 µM and 750 µM) and CoQ10 (10 µM and 25 µM) but not DX resulted neuroprotective compared to control against glutamate-mediated neurotoxicity (one-way ANOVA with Tukey posthoc test, p = 0.0012 and p =0.0012 respectively). [D,E] Neuroprotective effect of DMQ-loaded MSs against cytotoxic insult in R28 cell cultures. Treatment with DMQ-loaded MSs (20 mg MSs/mL) but not equivalent concentrations of non-loaded MSs only significantly (one-way ANOVA, *p* = 0.0061) reduced the susceptibility of these cells to glutamate-induced cytotoxicity.

3.4. Multiloaded MSs formulation inhibits RGC degeneration in the Morrison's model of ocular hypertension.

A well-established rodent model of experimental glaucoma was used to determine whether intravitreal injection of the multiloaded (DMQ) MSs had neuroprotective efficacy *in vivo*. Peak IOP was recorded one day after OHT induction and IOP elevation was maintained for at least 7 days after induction in all groups (Table 3 & Fig.6F). No significant change in IOP was observed in contralateral eyes. Intravitreal administration of the different treatments (empty-MSs, DMQ-MSs and physical mixture of MSs) had no effect on IOP profiles compared to OHT only eyes, suggesting that treatments did not affect IOP and that any neuroprotective effects observed were IOP independent.

Table 3

Mean IOP measurements and integral IOP (± SD) for each treatment group in this study.

Time post OHT induction (days)	OHT only	OHT (Co-eye)	OHT+Empty-MSs	OHT+Empty-MSs (co-eye)	OHT+DMQ-MSs	OHT+DMQ-MSs (co-eye)	OHT+Mixture of MSs	OHT+Mixture of MSs (co-eye)
0	10.03 (0.40)	10.02 (0.13)	10.18 (0.16)	10.34 (0.22)	10.40 (0.61)	10.30 (0.32)	10.30 (0.34)	10.00 (0.47)
1	25.46 (3.11)	10.95 (1.29)	22.70 (1.43)	10.10 (0.41)	25.70 (5.82)	10.25 (0.65)	24.56 (3.57)	10.66 (0.72)
7	19.94 (3.44)	10.48 (0.95)	20.32 (2.73)	10.28 (0.60)	20.30 (3.64)	10.43 (1.06)	18.02 (0.84)	10.22 (0.63)
14	14.20 (3.07)	11.78 (1.14)	14.88 (1.29)	10.78 (0.53)	14.60 (2.56)	10.85 (1.00)	15.92 (3.06)	11.44 (0.63)
21	12.34 (1.36)	10.80 (0.79)	13.01 (2.19)	10.56 (0.70)	12.45 (0.10)	10.95 (1.40)	15.62 (3.37)	11.24 (1.17)
Integral IOP (mmHg/day)	366.34 (23.65)	225.56 (16.36)	366.34 (32.24)	219.8 (5.25)	372.9 (45.06)	223.1 (16.17)	374.36 (24.82)	228.18 (4.60)

RGC loss due to increase of IOP was determined histologically by whole-retinal flat mounts immunolabeled with anti-Brn3a antibody (as example: Fig. 6Ai Naïve whole retina illustration). Figures from 6Aii to 6E show the RGC distribution from sections of Naive [Aii], OHT only [B], Empty MSs[C], Mixture MSs [D] and DMQ-MSs [E] from equivalent distances from the ONH in the retinal whole-mounts. Quantification of whole RGC populations was completed using an automated script as previously described [41]. Linear regression analysis (R version 3.3.1, eq. 2) was used to evaluate the efficacy of different treatments in the rodent OHT model with RGC density (cells/mm^2) as the dependent variable (y) and treatment group as the independent variables (β_T) with categories OHT only (intercept, β_0), Naïve retina, Drug loaded MSs, empty MSs and mixtures comprising three single-drug loaded MSs. The results of the regression analysis indicated the treatment group predictors explained 58.4% of the variance in RGC density ($R^2 = .50$, $F(4,19)=6.677$, $p=0.01565$). Compared to OHT only group ($\beta_0 = 1253 \pm 76$ cells/mm^2, $p < 0.001$) It was found that application of drug loaded MSs significantly preserved RGC density ($\beta_{T1} = 287 \pm 108$ cells/mm^2, *$p = 0.0155$), to a comparable extent as the naïve retina control group ($\beta_{T2}= 280 \pm 98$ cells/mm^2, *$p = 0.0104$). Administration of drug empty MSs ($\beta_{T3} = 4 \pm 102$ cells/mm^2, $p = 0.97$) or combinations of single-drug loaded MSs ($\beta_{T4} = -101 \pm 102$ cells/mm2, $p = 0.34$) with a residual standard error (ε) of 152 cells/mm2 with 19 DF. Administration of drug empty MSs ($\beta_{T3} = 4 \pm 102$ cells/mm^2, $p = 0.97$) or combinations of single-drug loaded MSs ($\beta_{T4} = -101 \pm 102$ cells/mm^2, $p = 0.34$) had no significant preserving effect on RGC population with a residual standard error (ε) of 152 cells/mm^2 with 19 DF (Figure 5G).

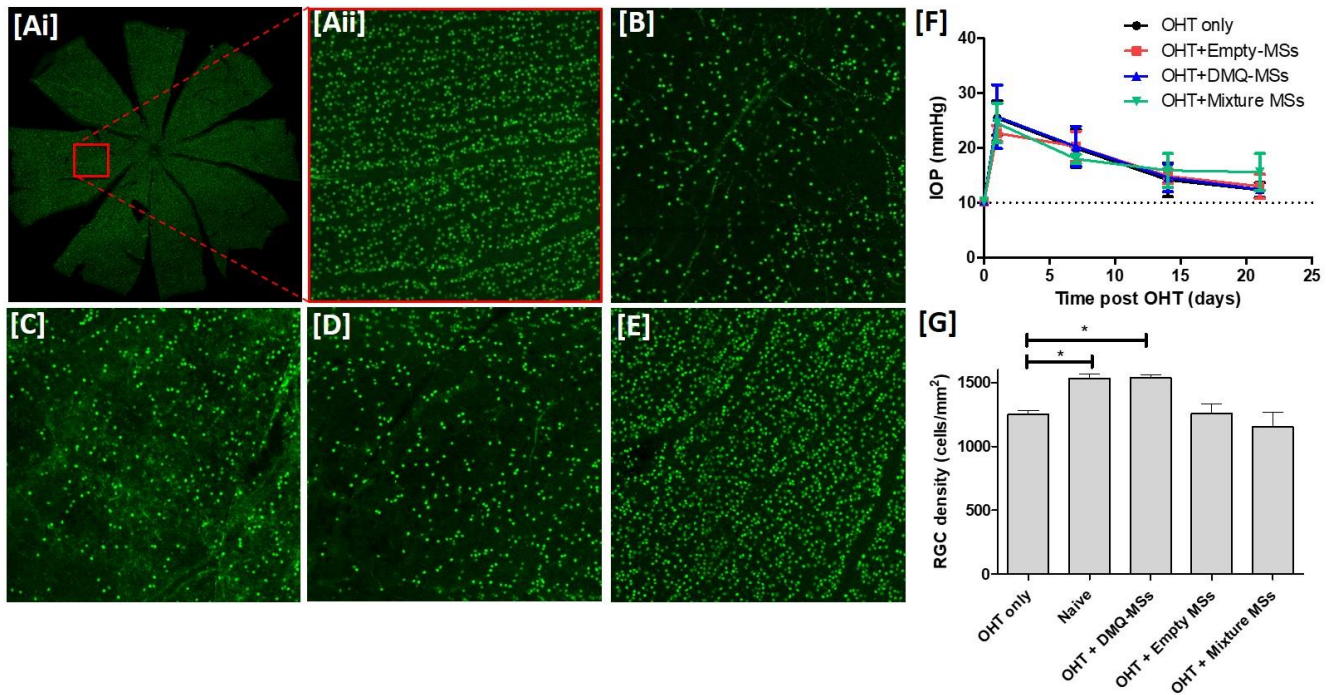$$y = \beta_0 + \beta_\tau x + \varepsilon \qquad \text{[eq. 2]}$$

Figure 6. Intravitreal DMQ-MSs treatment but not MSs Mixtures preserved RGC density in a well-established rodent model of Ocular Hypertension. Each red box is ~1 mm^2: [Ai] Naïve whole retina illustration [Aii] Illustration of RGC distribution from sections of Naive, [B] OHT only, [C] Empty MSs [D] Mixture MSs [E] DMQ-MSs treated retinal whole-mounts taken from equivalent distances from the ONH. [F] Treatment of eyes with intravitreal administration of Empty-MSs, DMQ-MSs or the mixture of MSs did not significantly alter the IOP profiles compared on OHT induction (two-way repeated measures ANOVA with Bonferroni post-test versus OHT model, p > 0.05) suggesting any neuroprotective activity of treatments was a result of IOP independent effects. Results are mean ± SD. [G] Whole retinal RGC density measurements indicate that while OHT induction ($\beta 0 = 1253 \pm 76$ cells/mm2, $p < 0.001$), empty MSs ($\beta \tau 3 = 4 \pm 102$ cells/mm2, $p = 0.97$) or combinations of single-drug loaded MSs ($\beta \tau 4 = -101 \pm 102$ cells/mm2, $p = 0.34$) caused a significant reduction in RGC density, RGC loss was preserved by an intravitreal administration of DMQ-MSs ($\beta \tau 1 = 287 \pm 108$ cells/mm2, *$p = 0.0155$), to a comparable extent as the naïve retina control group ($\beta \tau 2 = 280 \pm 98$ cells/mm2, *p

4. Discussion

Glaucoma is a worldwide leading cause of irreversible vision loss[46]. Although the exact mechanism of glaucoma pathology is debatable,[47] a hallmark of this disease is RGC degeneration that leads to vision deficit or loss[48]. Thus, there is an imperative need to develop RGC-targeted therapies that can be conveniently delivered providing via a long-term sustained drug release [49]. As the RGC degeneration occurs by different pathways, the present work suggests for the first time a beneficial role of a combination of three different neuroprotectants with anti-inflammatory and antioxidant activity (DX,

MEL, and CoQ10) formulated as a multi-loaded microparticulate PLGA system (DMQ-MSs) in reducing RGC loss in an experimental glaucomatous model. This multi-IODDS resulted more effective than the administration of a mixture of MSs loaded with the three drugs separately (MSsmix). As far as we are aware, this is the first co-delivery study for incorporating three neuroprotective agents into a single carrier system for the posterior segment of the eye.

High production efficiency yields (> 72%) and drug loading efficiencies (> 61%) were achieved in each case. DX encapsulation efficiency slightly decreased (~20%) in the multiloaded MSs compared to the single one drug formulation suggesting some competition for drug loading sites. The competition might be solved by the addition of co-solvents like ethanol into the inner polymeric solution. This technological strategy has been already reported by other authors [50-52]. However, since DMQ-MSs formulation contains three different drugs, this technology-based improvement would require optimization procedures.

Multi-loaded and single loaded MSs exhibited a homogeneous particle size (20 – 38 µm), with spherical morphology and were found to be suitable for its injection as a suspension through needles typically used for intravitreal administration (25G-32G) [53, 54]. Scanning electron microscopy images of CoQ10 loaded MSs and multi loaded-MSs revealed the presence of pores on the particles' rough surfaces. This fact has been previously explained as consequence of the rapid removal of organic solvent during elaboration procedure and to the encapsulation process characteristic of this poor soluble drug [55, 56]. According to the images observed by transmission electron microscopy, the inner structure of the multi loaded-MSs correspond to a combination of the different entrapped drugs. Thus, a mixture of DX solid forms and small and large pores like those observed in fractured MSs of MEL and CoQ10 can be observed in the multi-loaded formulation (DMQ-MSs). The appearance of inner pores larger than the

ones on the surface lies on the different solidification rates occurring during the processes of microsphere's formation and maturation[57].

The inner structure is determined by the solidification rate of the polymer during the microparticle preparation process. A high polymer concentration, as the one used in the present work, involves a faster polymeric precipitation resulting in a matrix dense and a relatively porous inside. The nature of the entrapped drugs is also a critical factor since release is longer with decreasing water solubility of the drug [52]. Therefore, the morphology of the microparticles, as well as the low solubility of the active compounds (DX, MEL, CoQ10), contributed to high encapsulation efficiencies and a prolonged release profile.

Additional characterization of MSs formulations was achieved using DSC. As expected, characteristic transitions of free drugs were present when these agents were assessed as physical mixtures with PLGA. DMQ-MSs thermogram, however, lost or reduced these characteristic peaks, providing evidence of their association with MSs polymeric matrix. This is further supported by the observation of a slight decrease in PLGA transition temperature in all formulations, probably due to the plasticiser effect of the small active molecules present and also to the micrometric size and high surface area of the particles [58]. Furthermore, the presence of the endothermic peak of DX in DX-MSs formulation could be attributed to the presence of DX crystals embedded in the MSs matrix, an expected result in accordance with the TEM images of these fractured microspheres. In addition, the disappearance of the CoQ10 endotherm in the thermogram of MSs containing CoQ10 regarding to the physical mixture, suggests the dissolution of CoQ10 in the polymeric organic solution during the production procedure [58]. Finally, contrary to the physical mixture (MEL plus PLGA), no free drug peaks were identified in the thermograms of MEL-MSs. This thermotropic variation would suggest that MEL was dispersed at molecular level inside the polymeric cavities, which might be attributed to the amphiphilic properties of the melatonin [59, 60] and could explain the TEM pictures

observed. DSC thermograms from DMQ-MSs revealed the presence of the melting peaks of DX and MEL, which might suggest the presence of part of these drugs in its solid form in the multi-loaded MSs formulation.

Multi-loaded microspheres provided simultaneous controlled co-delivery of the three therapeutics agents. The release rate of CoQ10 and DX from DMQ-MSs resulted in two (0.63 µg/mg MSs/day) and around three-fold (0.60 µg/mg MSs/day) higher respectively compared to single loaded particles. These findings could be explained by the lower polymer/mg MSs ratio in the multi-loaded particles. In contrast, the delivery of MEL resulted in significantly slower release rates (1.66 µg/mg MSs/day) than single loaded microspheres. A possible explanation for this is that the presence of very poorly soluble substances (such as CoQ10) can modulate the release of other more soluble compounds from a combined formulation [61]. Furthermore, the presence of MEL crystals in DMQ-MSs suggested by DSC studies may explain the release rate reduction; future studies will seek to confirm these hypotheses.

The neuroprotective activity of DMQ-MSs formulations were assessed using an *in vitro* glutamate-mediated neurotoxicity model in an immortalised neuronal cell line (R28). Results suggest that CoQ10 and MEL treatments were significantly protective against this insult. Glutamate mediated neurotoxicity in the retina is considered as one of the factors contributing to glaucoma pathogenesis [47, 62-64]. Neuronal vulnerability to glutamate has been attributed to mitochondrial membrane depolarization triggering a profound drop of intracellular ATP level and ROS generation [65, 66]. CoQ10 may help to the maintain mitochondrial membrane potential and so inhibit the opening of the mitochondrial permeability transition pore (PTP) which may lead to apoptosis induction [67]. Furthermore, it has been suggested that CoQ10 may also contribute to the reduction in expression of the glutamate binding receptor (N-methyl-D-aspartate receptor) subunits (NR1 and NR2A) in a mouse model of glaucoma [68]. We postulate

that these protective activities of CoQ10 work in conjunction with its well documented antioxidant activity [35] to protect R28 cells against glutamate-induced cell death.

The ability of MEL to inhibit glutamate neurotoxicity has been previously attributed to the reduction of oxidative stress via multiple processes [69]. MEL has been reported to act both as a direct free radical scavenger [70], and as an indirect antioxidant through the stimulation of antioxidant enzymes such as Superoxide dismutase [71]. MEL also promotes the synthesis of glutathione, an essential intracellular antioxidant [72], and it is able to increase the efficiency of the mitochondrial electron transport chain (ETC) thereby lowering electron leakage and reducing free radical generation [73, 74]. This study provides additional evidence to suggest that MEL is protective against glutamate-induced neurotoxicity and these findings are in agreement with those obtained by other groups [68, 75].

The *in vitro* experiments demonstrated no benefit of dexamethasone treatment in preserving cell function in vitro. However, the in vitro system does not model the full in vivo environment with multiple cell types at different levels. Our in vitro model consisted only of R28 cells and no microglia or astrocytes. We were therefore not expecting a neuroprotective effect with little expectation even for an immunemodulatory effect either, but wanted to be sure there was no toxicity. In any case inflammation events occurring within the in vivo environment of retinal degenerative diseases as we described in the introduction.

The DMQ-MSs formulation was assessed *in vivo* using a well-established rodent model of ocular hypertension (OHT) [76-78]. Intravitreal administration of 0.1 mg DMQ-MSs was compared to a physical mixture of single drug loaded MSs (0.23 mg) containing the same amount of active drug substances, empty MSs, an OHT only (untreated) group and naïve controls (No OHT or treatment). Three weeks after OHT induction, RGCs survival was quantified histologically from retinal whole mounts using Brn3a+ labelling as previously described [41]. Intravitreal administration of DMQ-MSs was found to

significantly promote RGCs survival compared to administration of empty MSs. Although the amount of drug release is low, particularly in the case of CoQ10, the simultaneous delivery of the three drugs resulted in a significant neuroprotective activity. The efficacy of low amounts released from PLGA microsystems loaded with neuroprotective agents has been already reported [61, 79-81].

Interestingly, administration of a mixture of MSs loaded with the three drugs separately (MSsmix) was found to be mildly neurotoxic. This may be related to the MSsmix formulations requiring a higher concentration of MSs particles than DMQ-MSs (0.23 mg vs 0.1 mg respectively), which may contribute to retinal toxicity. In support of this hypothesis, we previously reported that intravitreal injection of 0.5 mg of PLGA but not 0.1 mg PLGA induced retinal stress and neuronal cell dysfunctions in rats [23].

In the present work, a multi-therapy approach comprising DX, MEL and CoQ10 was chosen in order to target multiple pathways of neuronal degeneration simultaneously [12].

Corticosteroids has been suggested to induce neuroprotection by indirectly modulating microglia activity [82]. Furthermore, corticosteroid anti-inflammatory and immunosuppressive effects are thought to modulate the production of neurotoxic substances by microglial and the rate of phagocytosis of apoptotic neurons. [83] The neuroprotective effects of melatonin and coenzyme Q10 in the retina are based on their well-documented antioxidant activity and mitochondrial protection, which could prevent development and progression of neurodegeneration [29, 84].

MEL has demonstrated to protect retinal ganglion cells against apoptosis in a *in vivo* rodent model of nitric oxide induced retinal injury [30] and after acute injury intraorbital optic nerve transection or hypoxia [85, 86]. Interestedly, the protective effect of MEL is not only confined to neurons, as it may also elicit neuroprotection by acting on retinal glia, which is increasingly recognised to play an important role in the pathogenic cellular

processes of glaucoma [87]. Recently, we have also found that controlled delivery of MEL after a single intravitreal injection of MSs in combination with a neurotrophic factor (glial cell-line-derived neurotrophic factor, GDNF) promoted a rescue of the photoreceptors in rho (-/-) mice[24].

The neuroprotective effect of CoQ10 in RGCs has previously been suggested through the prevention of glutamate-induced apoptosis or inhibition of mitochondrial depolarization after topical administration in an IOP-induced transient ischemia rat model or in a UV-induced rat model of retinal damage respectively [67, 88]. In fact, topical instillation of this mitochondrial-targeted antioxidant was found to promote RGC neuroprotection in the same rodent model of ocular hypertension employed in the current study [36]. The mechanism of neuroprotection was attributed to the decrease of glutamate excitotoxicity and oxidative stress that preserve mtDNA content and Tfam/OXPHOS complex IV protein expression in the retina [68]. Similarly to MEL, the neuroprotective activity of CoQ10 has also been attributed to mitochondrial mediated modulation of retinal glial activation [89, 90].

Although several fixed combination therapies of antihypertensive drugs are currently in clinical practice, an equivalent neuroprotective combination therapy has not yet been clinically translated [91-93]. In summary, this paper presents a novel neuroprotective combination therapy combining an anti-inflammatory drug (DX) with two antioxidants (MEL and CoQ10). These drugs were delivered from a PLGA polymeric microcarrier (DMQ-MSs) which resulted in significant neuroprotection in a rodent model of RGC loss (ocular hypertension). Furthermore, the amount of polymer resulted lower than the one necessary for the physical mixture of microspheres resulting in a good tolerance of the formulation. Although the neuroprotective efficacy of other drug delivery systems has previously been reported [94-97], to the authors' knowledge, this is the first study to present an effective intraocular drug delivery system (IODDS) loaded with three drug cargo for the treatment of retinal degeneration.

Conclusion

This study presents a novel, effective and well-tolerated intraocular drug delivery system (IODDS) comprising PLGA polymeric microparticles for the co-delivery of three neuroprotective substances. This novel multi-therapy strategy allowed the co-incorporation of different drugs into a single microcarrier reduces the amount of biomaterial (PLGA) required for intraocular administration compared to equivalent dosing of single drug loaded formulations, so reducing the risk of PLGA associated retinal stress. Moreover, this IODDS provided the simultaneous release of the three active agents in a controlled fashion. *In vivo* efficacy studies revealed that the multi loaded IODDS could not only protected the RGCs from death, but also resulted in a higher efficacy than the physical mixture of MSs. These findings indicate that combination therapy using multi-loaded MSs may be a promising neuroprotective strategy for the treatment of multifactorial retinal diseases such as glaucoma.

Acknowledgements

References

[1] S.R. Flaxman, R.R.A. Bourne, S. Resnikoff, P. Ackland, T. Braithwaite, M.V. Cicinelli, A. Das, J.B. Jonas, J. Keeffe, J.H. Kempen, J. Leasher, H. Limburg, K. Naidoo, K. Pesudovs, A. Silvester, G.A. Stevens, N. Tahhan, T.Y. Wong, H.R. Taylor, S. Vision Loss Expert Group of the Global Burden of Disease, Global causes of blindness and distance vision impairment 1990-2020: a systematic review and meta-analysis, Lancet Glob Health, 5 (2017) e1221-e1234.
[2] M. Lawlor, H. Danesh-Meyer, L.A. Levin, I. Davagnanam, E. De Vita, G.T. Plant, Glaucoma and the brain: Trans-synaptic degeneration, structural change, and implications for neuroprotection, Surv Ophthalmol, (2017).
[3] R. Asaoka, H. Murata, M. Yanagisawa, Y. Fujino, M. Matsuura, T. Inoue, K. Inoue, J. Yamagami, The association between photoreceptor layer thickness measured by optical coherence tomography and visual sensitivity in glaucomatous eyes, PLoS One, 12 (2017) e0184064.
[4] B.S. Ashimatey, B.J. King, W.H. Swanson, Retinal putative glial alterations: implication for glaucoma care, Ophthalmic Physiol Opt, 38 (2018) 56-65.
[5] A.I. Ramirez, R. de Hoz, E. Salobrar-Garcia, J.J. Salazar, B. Rojas, D. Ajoy, I. Lopez-Cuenca, P. Rojas, A. Trivino, J.M. Ramirez, The Role of Microglia in Retinal Neurodegeneration: Alzheimer's Disease, Parkinson, and Glaucoma, Front Aging Neurosci, 9 (2017) 214.
[6] J. Qu, D. Wang, C.L. Grosskreutz, Mechanisms of retinal ganglion cell injury and defense in glaucoma, Exp Eye Res, 91 (2010) 48-53.
[7] A. Pascale, F. Drago, S. Govoni, Protecting the retinal neurons from glaucoma: lowering ocular pressure is not enough, Pharmacol Res, 66 (2012) 19-32.
[8] D.R. Anderson, S. Normal Tension Glaucoma, Collaborative normal tension glaucoma study, Curr Opin Ophthalmol, 14 (2003) 86-90.
[9] European Glaucoma Society Terminology and Guidelines for Glaucoma, 4th Edition - Chapter 3: Treatment principles and options Supported by the EGS Foundation: Part 1: Foreword; Introduction; Glossary; Chapter 3 Treatment principles and options, Br J Ophthalmol, 101 (2017) 130-195.
[10] M.T. Pardue, R.S. Allen, Neuroprotective strategies for retinal disease, Prog Retin Eye Res, (2018).
[11] C. Nucci, R. Russo, A. Martucci, C. Giannini, F. Garaci, R. Floris, G. Bagetta, L.A. Morrone, New strategies for neuroprotection in glaucoma, a disease that affects the central nervous system, Eur J Pharmacol, 787 (2016) 119-126.
[12] A. Baltmr, J. Duggan, S. Nizari, T.E. Salt, M.F. Cordeiro, Neuroprotection in glaucoma - Is there a future role?, Exp Eye Res, 91 (2010) 554-566.
[13] R. Russo, G.P. Varano, A. Adornetto, C. Nucci, M.T. Corasaniti, G. Bagetta, L.A. Morrone, Retinal ganglion cell death in glaucoma: Exploring the role of neuroinflammation, Eur J Pharmacol, 787 (2016) 134-142.
[14] C. McMonnies, Reactive oxygen species, oxidative stress, glaucoma and hyperbaric oxygen therapy, J Optom, 11 (2018) 3-9.
[15] G. Tezel, Oxidative stress in glaucomatous neurodegeneration: mechanisms and consequences, Prog Retin Eye Res, 25 (2006) 490-513.
[16] N. Cuenca, L. Fernandez-Sanchez, L. Campello, V. Maneu, P. De la Villa, P. Lax, I. Pinilla, Cellular responses following retinal injuries and therapeutic approaches for neurodegenerative diseases, Prog Retin Eye Res, 43 (2014) 17-75.
[17] B.G. Short, Safety evaluation of ocular drug delivery formulations: techniques and practical considerations, Toxicol Pathol, 36 (2008) 49-62.

[18] P. Mitchell, A systematic review of the efficacy and safety outcomes of anti-VEGF agents used for treating neovascular age-related macular degeneration: comparison of ranibizumab and bevacizumab, Curr Med Res Opin, 27 (2011) 1465-1475.

[19] I.B.-O. V. Andrés-Guerrero, P. Pastoriza, I.T. Molina-Martinez, Rocí. Herrero-Vanrell, Novel technologies for the delivery of ocular therapeutics in glaucoma, Journal of Drug Delivery Science and Technology, 42 (2017) 181-192.

[20] I. Bravo-Osuna, V. Andres-Guerrero, A. Arranz-Romera, S. Esteban-Perez, I.T. Molina-Martinez, R. Herrero-Vanrell, Microspheres as intraocular therapeutic tools in chronic diseases of the optic nerve and retina, Adv Drug Deliv Rev, (2018).

[21] X. Rong, W. Yuan, Y. Lu, X. Mo, Safety evaluation of poly(lactic-co-glycolic acid)/poly(lactic-acid) microspheres through intravitreal injection in rabbits, Int J Nanomedicine, 9 (2014) 3057-3068.

[22] I. Bravo-Osuna, V. Andres-Guerrero, P. Pastoriza Abal, I.T. Molina-Martinez, R. Herrero-Vanrell, Pharmaceutical microscale and nanoscale approaches for efficient treatment of ocular diseases, Drug Deliv Transl Res, 6 (2016) 686-707.

[23] M. Zhao, E. Rodriguez-Villagra, L. Kowalczuk, M. Le Normand, M. Berdugo, R. Levy-Boukris, I. El Zaoui, B. Kaufmann, R. Gurny, I. Bravo-Osuna, I.T. Molina-Martinez, R. Herrero-Vanrell, F. Behar-Cohen, Tolerance of high and low amounts of PLGA microspheres loaded with mineralocorticoid receptor antagonist in retinal target site, J Control Release, 266 (2017) 187-197.

[24] L.B. García-Caballero C., Arranz-Romera A., Molina-Martínez I.T., Bravo-Osuna I., Young M., Baranov P., Herrero-Vanrell R., Photoreceptor preservation induced by intravitreal controlled delivery of GDNF and GDNF/melatonin in rhodopsin knockout mice, Molecular Vision, 24 (2018) 733-745

[25] N.V. Saraiya, D.A. Goldstein, Dexamethasone for ocular inflammation, Expert Opin Pharmacother, 12 (2011) 1127-1131.

[26] G. Zhang, S. Liu, L. Yang, Y. Li, The role of Dexamethasone in clinical pharmaceutical treatment for patients with cataract surgery, Exp Ther Med, 15 (2018) 2177-2181.

[27] C.J. Brady, A.C. Villanti, H.A. Law, E. Rahimy, R. Reddy, P.C. Sieving, S.J. Garg, J. Tang, Corticosteroid implants for chronic non-infectious uveitis, Cochrane Database Syst Rev, 2 (2016) CD010469.

[28] P.O. Lundmark, S.R. Pandi-Perumal, V. Srinivasan, D.P. Cardinali, R.E. Rosenstein, Melatonin in the eye: implications for glaucoma, Exp Eye Res, 84 (2007) 1021-1030.

[29] P. Wongprayoon, P. Govitrapong, Melatonin as a mitochondrial protector in neurodegenerative diseases, Cell Mol Life Sci, 74 (2017) 3999-4014.

[30] A.W. Siu, G.G. Ortiz, G. Benitez-King, C.H. To, R.J. Reiter, Effects of melatonin on the nitric oxide treated retina, Br J Ophthalmol, 88 (2004) 1078-1081.

[31] S.A. Andrabi, I. Sayeed, D. Siemen, G. Wolf, T.F. Horn, Direct inhibition of the mitochondrial permeability transition pore: a possible mechanism responsible for anti-apoptotic effects of melatonin, FASEB J, 18 (2004) 869-871.

[32] G.P. Littarru, L. Tiano, Clinical aspects of coenzyme Q10: an update, Nutrition, 26 (2010) 250-254.

[33] P. Forsmark-Andree, C.P. Lee, G. Dallner, L. Ernster, Lipid peroxidation and changes in the ubiquinone content and the respiratory chain enzymes of submitochondrial particles, Free Radic Biol Med, 22 (1997) 391-400.

[34] A. Virmani, F. Gaetani, Z. Binienda, Effects of metabolic modifiers such as carnitines, coenzyme Q10, and PUFAs against different forms of neurotoxic insults: metabolic inhibitors, MPTP, and methamphetamine, Ann N Y Acad Sci, 1053 (2005) 183-191.

[35] J.D. Hernandez-Camacho, M. Bernier, G. Lopez-Lluch, P. Navas, Coenzyme Q10 Supplementation in Aging and Disease, Front Physiol, 9 (2018) 44.

[36] B.M. Davis, K. Tian, M. Pahlitzsch, J. Brenton, N. Ravindran, G. Butt, G. Malaguarnera, E.M. Normando, L. Guo, M.F. Cordeiro, Topical Coenzyme Q10 demonstrates mitochondrial-

mediated neuroprotection in a rodent model of ocular hypertension, Mitochondrion, 36 (2017) 114-123.

[37] G.M. Seigel, Review: R28 retinal precursor cells: the first 20 years, Mol Vis, 20 (2014) 301-306.

[38] J.C. Morrison, W.O. Cepurna, E.C. Johnson, Modeling glaucoma in rats by sclerosing aqueous outflow pathways to elevate intraocular pressure, Exp Eye Res, 141 (2015) 23-32.

[39] J.C. Morrison, DeFrank, M. P. & Van Buskirk, E. M. , Comparative microvascular anatomy of mammalian ciliary processes, IOVS, 28 (1987) 1325–1340.

[40] J.C. Morrison, C.G. Moore, L.M. Deppmeier, B.G. Gold, C.K. Meshul, E.C. Johnson, A rat model of chronic pressure-induced optic nerve damage, Exp Eye Res, 64 (1997) 85-96.

[41] B.M. Davis, L. Guo, J. Brenton, L. Langley, E.M. Normando, M.F. Cordeiro, Automatic quantitative analysis of experimental primary and secondary retinal neurodegeneration: implications for optic neuropathies, Cell Death Discov, 2 (2016) 16031.

[42] F.M. Nadal-Nicolas, M. Jimenez-Lopez, M. Salinas-Navarro, P. Sobrado-Calvo, J.J. Alburquerque-Bejar, M. Vidal-Sanz, M. Agudo-Barriuso, Whole number, distribution and co-expression of brn3 transcription factors in retinal ganglion cells of adult albino and pigmented rats, PLoS One, 7 (2012) e49830.

[43] K. Park, Controlled drug delivery systems: past forward and future back, J Control Release, 190 (2014) 3-8.

[44] K.K. Jain, Current status and future prospects of drug delivery systems, Methods Mol Biol, 1141 (2014) 1-56.

[45] R. Herrero-Vanrell, I. Bravo-Osuna, V. Andres-Guerrero, M. Vicario-de-la-Torre, I.T. Molina-Martinez, The potential of using biodegradable microspheres in retinal diseases and other intraocular pathologies, Prog Retin Eye Res, 42 (2014) 27-43.

[46] R.N. Weinreb, T. Aung, F.A. Medeiros, The pathophysiology and treatment of glaucoma: a review, JAMA, 311 (2014) 1901-1911.

[47] B.M. Davis, L. Crawley, M. Pahlitzsch, F. Javaid, M.F. Cordeiro, Glaucoma: the retina and beyond, Acta Neuropathol, 132 (2016) 807-826.

[48] R.W. Nickells, G.R. Howell, I. Soto, S.W. John, Under pressure: cellular and molecular responses during glaucoma, a common neurodegeneration with axonopathy, Annu Rev Neurosci, 35 (2012) 153-179.

[49] L. Zhao, G. Chen, J. Li, Y. Fu, T.A. Mavlyutov, A. Yao, R.W. Nickells, S. Gong, L.W. Guo, An intraocular drug delivery system using targeted nanocarriers attenuates retinal ganglion cell degeneration, J Control Release, 247 (2017) 153-166.

[50] R. Jeyanthi, Mehta, R. C., Thanoo, B. C., and DeLuca, P. P. , Effect of processing parameters on the properties of peptide containing PLGA microspheres, J. Microencapsulation, 14 (1997) 163-174.

[51] T.G. Park, Lee, H. Y., and Nam, Y. S., A new preparation method for protein loaded poly(D,L-lactic-co-cjlycolic acid) microspheres and protein release mechanism study, J. Controlled Release, 55 (1998) 181-191.

[52] Y. Yeo, K. Park, Control of encapsulation efficiency and initial burst in polymeric microparticle systems, Arch Pharm Res, 27 (2004) 1-12.

[53] R. Herrero-Vanrell, M.F. Refojo, Biodegradable microspheres for vitreoretinal drug delivery, Adv Drug Deliv Rev, 52 (2001) 5-16.

[54] V. Andres-Guerrero, M. Zong, E. Ramsay, B. Rojas, S. Sarkhel, B. Gallego, R. de Hoz, A.I. Ramirez, J.J. Salazar, A. Trivino, J.M. Ramirez, E.M. Del Amo, N. Cameron, B. de-Las-Heras, A. Urtti, G. Mihov, A. Dias, R. Herrero-Vanrell, Novel biodegradable polyesteramide microspheres for controlled drug delivery in Ophthalmology, J Control Release, 211 (2015) 105-117.

[55] L. Al Haushey, M.A. Bolzinger, C. Bordes, J.Y. Gauvrit, S. Briancon, Improvement of a bovine serum albumin microencapsulation process by screening design, Int J Pharm, 344 (2007) 16-25.

[56] P.R. Nepal, H.K. Han, H.K. Choi, Enhancement of solubility and dissolution of coenzyme Q10 using solid dispersion formulation, Int J Pharm, 383 (2010) 147-153.

[57] D.H. Paik, S.W. Choi, Entrapment of protein using electrosprayed poly(D,L-lactide-co-glycolide) microspheres with a porous structure for sustained release, Macromol Rapid Commun, 35 (2014) 1033-1038.

[58] E.S. Farboud, S.A. Nasrollahi, Z. Tabbakhi, Novel formulation and evaluation of a Q10-loaded solid lipid nanoparticle cream: in vitro and in vivo studies, Int J Nanomedicine, 6 (2011) 611-617.

[59] T. Musumeci, C. Bucolo, C. Carbone, R. Pignatello, F. Drago, G. Puglisi, Polymeric nanoparticles augment the ocular hypotensive effect of melatonin in rabbits, Int J Pharm, 440 (2013) 135-140.

[60] S.D.a.U. Subuddhi, Controlled delivery of dexamethasone to the intestine from poly(vinyl alcohol)–poly(acrylic acid) microspheres containing drug-cyclodextrin complexes: influence of method of preparation ofinclusion complex, RSC Advances, 4 (2014) 24222–24231.

[61] P.J. Checa-Casalengua, C. Bravo-Osuna, I. Tucker, B. A. Molina-Martinez, I. T. Young, M. J., Herrero-Vanrell, R., Retinal ganglion cells survival in a glaucoma model by GDNF/Vit E PLGA microspheres prepared according to a novel microencapsulation procedure, J Control Release, 156 (2011) 92-100.

[62] L. Guo, T.E. Salt, A. Maass, V. Luong, S.E. Moss, F.W. Fitzke, M.F. Cordeiro, Assessment of neuroprotective effects of glutamate modulation on glaucoma-related retinal ganglion cell apoptosis in vivo, Invest Ophthalmol Vis Sci, 47 (2006) 626-633.

[63] R.L. Gross, S.H. Hensley, F. Gao, S.M. Wu, Retinal ganglion cell dysfunction induced by hypoxia and glutamate: potential neuroprotective effects of beta-blockers, Surv Ophthalmol, 43 Suppl 1 (1999) S162-170.

[64] X. Luo, V. Heidinger, S. Picaud, G. Lambrou, H. Dreyfus, J. Sahel, D. Hicks, Selective excitotoxic degeneration of adult pig retinal ganglion cells in vitro, Invest Ophthalmol Vis Sci, 42 (2001) 1096-1106.

[65] J.K. Sandhu, S. Pandey, M. Ribecco-Lutkiewicz, R. Monette, H. Borowy-Borowski, P.R. Walker, M. Sikorska, Molecular mechanisms of glutamate neurotoxicity in mixed cultures of NT2-derived neurons and astrocytes: protective effects of coenzyme Q10, J Neurosci Res, 72 (2003) 691-703.

[66] S. Vishnoi, S. Raisuddin, S. Parvez, Glutamate Excitotoxicity and Oxidative Stress in Epilepsy: Modulatory Role of Melatonin, J Environ Pathol Toxicol Oncol, 35 (2016) 365-374.

[67] L. Papucci, N. Schiavone, E. Witort, M. Donnini, A. Lapucci, A. Tempestini, L. Formigli, S. Zecchi-Orlandini, G. Orlandini, G. Carella, R. Brancato, S. Capaccioli, Coenzyme q10 prevents apoptosis by inhibiting mitochondrial depolarization independently of its free radical scavenging property, J Biol Chem, 278 (2003) 28220-28228.

[68] D. Lee, M.S. Shim, K.Y. Kim, Y.H. Noh, H. Kim, S.Y. Kim, R.N. Weinreb, W.K. Ju, Coenzyme Q10 inhibits glutamate excitotoxicity and oxidative stress-mediated mitochondrial alteration in a mouse model of glaucoma, Invest Ophthalmol Vis Sci, 55 (2014) 993-1005.

[69] R.J. Reiter, D.X. Tan, J.C. Mayo, R.M. Sainz, J. Leon, Z. Czarnocki, Melatonin as an antioxidant: biochemical mechanisms and pathophysiological implications in humans, Acta Biochim Pol, 50 (2003) 1129-1146.

[70] R.J. Reiter, D.X. Tan, C. Osuna, E. Gitto, Actions of melatonin in the reduction of oxidative stress. A review, J Biomed Sci, 7 (2000) 444-458.

[71] I. Antolin, B. Obst, S. Burkhardt, R. Hardeland, Antioxidative protection in a high-melatonin organism: the dinoflagellate Gonyaulax polyedra is rescued from lethal oxidative stress by strongly elevated, but physiologically possible concentrations of melatonin, J Pineal Res, 23 (1997) 182-190.

[72] Y. Urata, S. Honma, S. Goto, S. Todoroki, T. Iida, S. Cho, K. Honma, T. Kondo, Melatonin induces gamma-glutamylcysteine synthetase mediated by activator protein-1 in human vascular endothelial cells, Free Radic Biol Med, 27 (1999) 838-847.

[73] J.C. Mayo, R.M. Sainz, P. Gonzalez-Menendez, D. Hevia, R. Cernuda-Cernuda, Melatonin transport into mitochondria, Cell Mol Life Sci, 74 (2017) 3927-3940.

[74] R.J. Reiter, S. Rosales-Corral, D.X. Tan, M.J. Jou, A. Galano, B. Xu, Melatonin as a mitochondria-targeted antioxidant: one of evolution's best ideas, Cell Mol Life Sci, 74 (2017) 3863-3881.

[75] P. Patino, E. Parada, V. Farre-Alins, S. Molz, R. Cacabelos, J. Marco-Contelles, M.G. Lopez, C.I. Tasca, E. Ramos, A. Romero, J. Egea, Melatonin protects against oxygen and glucose deprivation by decreasing extracellular glutamate and Nox-derived ROS in rat hippocampal slices, Neurotoxicology, 57 (2016) 61-68.

[76] E. Sanchez-Lopez, M.A. Egea, B.M. Davis, L. Guo, M. Espina, A.M. Silva, A.C. Calpena, E.M.B. Souto, N. Ravindran, M. Ettcheto, A. Camins, M.L. Garcia, M.F. Cordeiro, Memantine-Loaded PEGylated Biodegradable Nanoparticles for the Treatment of Glaucoma, Small, 14 (2018).

[77] A. Dibas, M.H. Yang, S. He, J. Bobich, T. Yorio, Changes in ocular aquaporin-4 (AQP4) expression following retinal injury, Mol Vis, 14 (2008) 1770-1783.

[78] M. Liu, L. Guo, T.E. Salt, M.F. Cordeiro, Dendritic changes in rat visual pathway associated with experimental ocular hypertension, Curr Eye Res, 39 (2014) 953-963.

[79] M.S. Ward, A. Khoobehi, E.B. Lavik, R. Langer, M.J. Young, Neuroprotection of retinal ganglion cells in DBA/2J mice with GDNF-loaded biodegradable microspheres, J Pharm Sci, 96 (2007) 558-568.

[80] C. Jiang, M.J. Moore, X. Zhang, H. Klassen, R. Langer, M. Young, Intravitreal injections of GDNF-loaded biodegradable microspheres are neuroprotective in a rat model of glaucoma, Mol Vis, 13 (2007) 1783-1792.

[81] C. Andrieu-Soler, A. Aubert-Pouessel, M. Doat, S. Picaud, M. Halhal, M. Simonutti, M.C. Venier-Julienne, J.P. Benoit, F. Behar-Cohen, Intravitreous injection of PLGA microspheres encapsulating GDNF promotes the survival of photoreceptors in the rd1/rd1 mouse, Mol Vis, 11 (2005) 1002-1011.

[82] P.D. Drew, J.A. Chavis, Inhibition of microglial cell activation by cortisol, Brain Res Bull, 52 (2000) 391-396.

[83] L. Vardimon, I. Ben-Dror, N. Avisar, A. Oren, L. Shiftan, Glucocorticoid control of glial gene expression, J Neurobiol, 40 (1999) 513-527.

[84] I.P. Hargreaves, Coenzyme Q10 as a therapy for mitochondrial disease, Int J Biochem Cell Biol, 49 (2014) 105-111.

[85] E. Kilic, D.M. Hermann, S. Isenmann, M. Bahr, Effects of pinealectomy and melatonin on the retrograde degeneration of retinal ganglion cells in a novel model of intraorbital optic nerve transection in mice, J Pineal Res, 32 (2002) 106-111.

[86] C. Kaur, V. Sivakumar, R. Robinson, W.S. Foulds, C.D. Luu, E.A. Ling, Neuroprotective effect of melatonin against hypoxia-induced retinal ganglion cell death in neonatal rats, J Pineal Res, 54 (2013) 190-206.

[87] G. Tezel, The immune response in glaucoma: a perspective on the roles of oxidative stress, Exp Eye Res, 93 (2011) 178-186.

[88] C. Nucci, R. Tartaglione, A. Cerulli, R. Mancino, A. Spano, F. Cavaliere, L. Rombola, G. Bagetta, M.T. Corasaniti, L.A. Morrone, Retinal damage caused by high intraocular pressure-induced transient ischemia is prevented by coenzyme Q10 in rat, Int Rev Neurobiol, 82 (2007) 397-406.

[89] L. Jing, M.T. He, Y. Chang, S.L. Mehta, Q.P. He, J.Z. Zhang, P.A. Li, Coenzyme Q10 protects astrocytes from ROS-induced damage through inhibition of mitochondria-mediated cell death pathway, Int J Biol Sci, 11 (2015) 59-66.

[90] M. Bhardwaj, A. Kumar, Neuroprotective mechanism of Coenzyme Q10 (CoQ10) against PTZ induced kindling and associated cognitive dysfunction: Possible role of microglia inhibition, Pharmacol Rep, 68 (2016) 1301-1311.

[91] G. Hollo, J. Vuorinen, J. Tuominen, T. Huttunen, A. Ropo, N. Pfeiffer, Fixed-dose combination of tafluprost and timolol in the treatment of open-angle glaucoma and ocular hypertension: comparison with other fixed-combination products, Adv Ther, 31 (2014) 932-944.

[92] G. Hollo, F. Topouzis, R.D. Fechtner, Fixed-combination intraocular pressure-lowering therapy for glaucoma and ocular hypertension: advantages in clinical practice, Expert Opin Pharmacother, 15 (2014) 1737-1747.

[93] S. Guven Yilmaz, C. Degirmenci, Y.E. Karakoyun, E. Yusifov, H. Ates, The efficacy and safety of bimatoprost/timolol maleate, latanoprost/timolol maleate, and travoprost/timolol maleate fixed combinations on 24-h IOP, Int Ophthalmol, 38 (2018) 1425-1431.

[94] M. Aihara, M. Adachi, H. Matsuo, T. Togano, T. Fukuchi, N. Sasaki, J.A.C.S. groupdagger, Additive effects and safety of fixed combination therapy with 1% brinzolamide and 0.5% timolol versus 1% dorzolamide and 0.5% timolol in prostaglandin-treated glaucoma patients, Acta Ophthalmol, 95 (2017) e720-e726.

[95] J. Rodriguez Villanueva, I. Bravo-Osuna, R. Herrero-Vanrell, I.T. Molina Martinez, M. Guzman Navarro, Optimising the controlled release of dexamethasone from a new generation of PLGA-based microspheres intended for intravitreal administration, Eur J Pharm Sci, 92 (2016) 287-297.

[96] L.G. Martins, N.M. Khalil, R.M. Mainardes, Plga Nanoparticles and Polysorbate-80-Coated Plga Nanoparticles Increase in the Vitro Antioxiant Activity of Melatonin, Curr Drug Deliv, (2017).

[97] S. Kumar, R. Rao, A. Kumar, S. Mahant, S. Nanda, Novel Carriers for Coenzyme Q10 Delivery, Curr Drug Deliv, 13 (2016) 1184-1204.